

A data-driven approach to determine dipole moments of diatomic molecules

Xiangyue Liu,¹ Gerard Meijer,¹ and Jesús Pérez-Ríos¹
Fritz-Haber-Institut der Max-Planck-Gesellschaft, Faradayweg 4-6, 14195 Berlin, Germany

(Dated: 28 July 2020)

We present a data-driven approach for the prediction of the electric dipole moment of diatomic molecules, which is one of the most relevant molecular properties. In particular, we apply Gaussian process regression to a novel dataset to show that dipole moments of diatomic molecules can be learned, and hence predicted, with a relative error $\lesssim 5\%$. The dataset contains the dipole moment of 162 diatomic molecules, the most exhaustive and unbiased dataset of dipole moments up to date. Our findings show that the dipole moment of diatomic molecules depends on atomic properties of the constituents atoms: electron affinity and ionization potential, as well as on (a feature related to) the first derivative of the electronic kinetic energy at the equilibrium distance.

I. INTRODUCTION

The study of relationships between spectroscopic constants is a traditional topic in chemical physics since the pioneering work of Kratzer and Mecke, among others¹⁻⁶ and is beautifully summarized by Varshini.^{7,8} Recently, we have shown that some spectroscopic constants are universally related,⁹ i.e., the relationships between them are independent of the nature of the molecular bond. However, the electric dipole moment of a molecule, despite being an essential molecular property, has not been considered in previous studies about relationships between spectroscopic constants. Only recently, there have been some efforts towards the understanding of the dipole moment in terms of molecular spectroscopic constants. As a result, it has been found by Hou and Bernath that the expression for the dipole moment, d , taught in elementary chemistry courses

$$d = qR_e, \quad (1)$$

where q is the effective charge and R_e denotes the equilibrium bond length of the molecule, does not capture the proper physics of the dipole moment in many molecules.^{10,11} They also demonstrated that the dipole moment of some molecules can be predicted from the effective charge (obtained from quantum chemistry calculations) and spectroscopic constants of molecules.

In the 2000s the big data-driven science paradigm emerged in the scientific community.¹² In this new paradigm, machine learning techniques are among the most prominent tools to assess scientific knowledge. To be precise, adequately formatted data are used to identify unexpected correlations and to predict observables based on patterns and trends of the data. When applied to physics, this novel paradigm lets nature speak up through hidden and intriguing correlations that lead to the formulation of new questions beyond a specific physical model. In particular, in chemical physics, as recently shown, data-driven approaches bring a new perspective to solve some of the most delicate problems of the field.¹³⁻¹⁶

In this paper, we present a data-driven approach to dipole moments of diatomic molecules and its relationship with spectroscopic constants. We show that, after compiling the most

exhaustive list of dipole moments for diatomics up to date (to the best of our knowledge) into a dataset, it is possible to learn the dipole moment of diatomic molecules based upon atomic and molecular properties with an error $\lesssim 5\%$. The number of molecules in our dataset, classified by the type of the constituent atoms, is given in Fig. 1. Our results reveal that it is not possible to predict the dipole moment of a molecule solely from atomic properties, although this is feasible for the spectroscopic constants,⁹ but that it is necessary to include molecular features. The molecular spectroscopic constants are needed in a combination that describes the force on the electrons at the equilibrium distance, i.e. in a combination that has the same functional dependence as the first derivative of the electronic kinetic energy at the equilibrium distance.

II. AN OVERVIEW ON THE NATURE OF THE ELECTRIC DIPOLE MOMENT OF MOLECULES

The study of the nature of the electric dipole moment of molecules is a traditional topic in quantum chemistry that has fascinated the chemical physics community for almost a century by now. The first explanation of the nature of the electric dipole moment of molecules is due to Pauling in the 1930s¹⁷. In particular, after studying hydrogen halide molecules, Pauling proposed that the dipole moment of a molecule is correlated with the relevance of the ionic structure with respect to the covalent one at the equilibrium bond length of the molecule. In this model, the dipole moment is a consequence of the charge transfer between the atoms within the molecule. Therefore, the larger the charge transfer, the bigger the dipole moment is. The charge transfer is quantized by the ionic character (IC), which is given by

$$\text{IC} = \frac{d}{eR_e}, \quad (2)$$

where e is the electron charge. Comparing Eqs. (2) and (1), it is clear that the ionic character is equivalent to the effective charge, q , placed at the center of each of the atoms forming the molecule, as prescribed by Eq. (1). However, Pauling's model does not predict 100% of ionic character for molecules that are fully ionic, like the alkali metal halides. Despite the

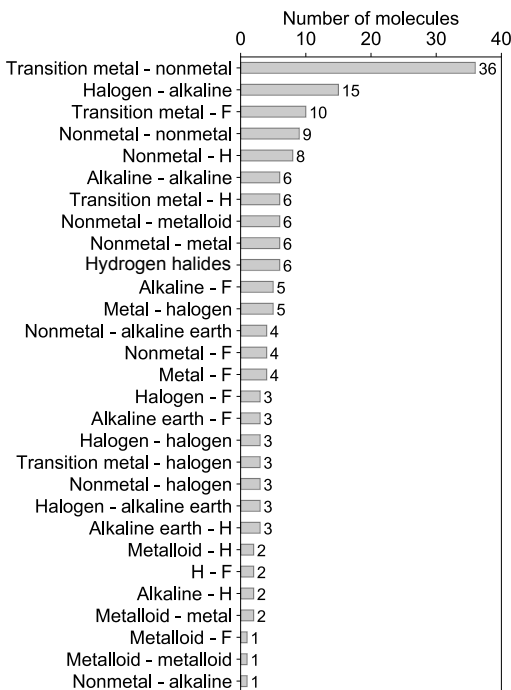


FIG. 1. Molecules in the whole dataset classified by the types of their constituent atoms.

slight inaccuracy of Pauling’s model in predicting dipole moments, it is worth emphasizing that Pauling realized that the dipole moment of a molecule must be related to other molecular properties through the molecular bond.

The next step towards understanding the electric dipole moment was the introduction of a new concept: the homopolar dipole moment, d_h , by Mulliken. In particular, Mulliken realized that because the atomic orbitals are different in size, the overlap between those leads to a charge displacement with respect to the midpoint of the equilibrium bond length, which affects the electric dipole moment of the molecule¹⁸. Furthermore, Mulliken noticed that the asymmetry in the charge distribution of hybrid orbitals causes the so-called atomic dipole moment, d_a . The models of Mulliken and Pauling were summarized and further developed by Coulson¹⁹, who proposed the ultimate expression for the dipole moment of a diatomic molecule as

$$d = eR_e + d_a + d_h + d_p, \quad (3)$$

where d_p is the contribution due to the polarization of the atomic orbitals to the dipole moment of the molecule. One has to realise that Eq. (3), although being more precise than Eq. (1), requires the input from quantum chemistry calculations. For a summary on the Pauling and Mulliken models, we recommend the comprehensive review of Klessinger.²⁰

The models of Pauling and Mulliken have been accepted by the physical chemistry community and taught in elementary chemistry courses for a long time, despite the fact that neither one of those is fully satisfactory. Recently, Hou and

Bernath^{10,11}, after studying the experimentally determined dipole moments of an extensive group of molecules and using quantum chemistry calculations, have suggested that the electric dipole moment of a molecule should be given as

$$d = qR_d \quad (4)$$

where q is the effective charge and R_d is an effective length that depends on fundamental spectroscopic constants of the molecule with $R_d < R_e$. Both Eq. (4) and Eq. (3) rely on the input of quantum chemistry calculations, in particular on the results from a natural bond orbital analysis. Therefore, the electric dipole moment of diatomic molecules still lacks a satisfactory and accurate explanation in terms of fundamental spectroscopic constants.

III. MACHINE LEARNING MODEL

A. Gaussian process regression

Finding relationships of the dipole moment with spectroscopic constants can be viewed as a regression problem, where the goal is to learn the mapping from the input atomic and molecular features \mathbf{x} onto the target property, y , which in this case is the electric dipole moment, by a function $y = f(\mathbf{x})$. In the present work, we use Gaussian process regression (GPR) to approximate the function $f(\mathbf{x})$. As a non-parametric probabilistic method, GPR does not presume a functional form of $f(\mathbf{x})$ before observing the data. Instead, it infers a Gaussian distribution of functions over function space by a Gaussian process^{21,22}

$$f(\mathbf{x}) \sim \text{GP}(m(\mathbf{x}), k(\mathbf{x}, \mathbf{x}')), \quad (5)$$

determined by a mean function, $m(\mathbf{x})$, and a kernel (covariance) function, $k(\mathbf{x}, \mathbf{x}')$. The prior, $p(f|\mathbf{x})$, spanning in the function space, after exposed to the observations, is constrained into a posterior, $p(f|\mathbf{x}, y)$, based on the Bayes theorem. The predictions, y^* , can then be made for new input atomic and molecular features, \mathbf{x} , through the posterior.

The kernel function, $k(\mathbf{x}, \mathbf{x}')$, captures the smoothness of the response and intrinsically encodes the behaviour of the model acting on the input. The kernel functions can be chosen by presuming the behaviour of the response to the input feature by observing the data. Its functional form and the possible hyperparameters can also be determined by a cross-validation (CV)²³.

B. Model evaluation

In learning the dipole moments, the dataset is divided into training and test sets. As a data-driven approach, GPR learns the relationship between the input features and dipole moments by observing the training set, while the predictive performance of the GPR models is examined with the test set.

In this work, 20 molecules are used in the test set, while the rest are used in the training set. For the training/test splitting, the dataset is first stratified into 20 strata based on the dipole moments' true values. A Monte Carlo (MC) approach is then performed to select the 20 test data from the dataset randomly. In each MC step, a GPR model is trained based on the training set with 5-fold cross-validation. The generalization performance of the model is then evaluated with the test set. In the end, the mean and standard deviation (STD) of the test-set errors are reported in this work, obtained from 1000 MC training/test splittings. Details about this MC approach will be discussed elsewhere.²⁴

The performance evaluation of the GPR models is carried out through three different estimators:

- The mean absolute error (MAE) defined as

$$\text{MAE} = \frac{1}{N} \sum_{i=1}^N |y_i - y_i^*|, \quad (6)$$

where y_i are the true values of dipole moments, y_i^* are the predictions, and N is the number of observations in the dataset.

- The root mean square error (RMSE), which reads as

$$\text{RMSE} = \sqrt{\frac{1}{N} \sum_{i=1}^N (y_i - y_i^*)^2}. \quad (7)$$

- The normalized error, r_E , defined as the ratio of the RMSE to the range of the data

$$r_E = \frac{\text{RMSE}}{y_{\max} - y_{\min}}. \quad (8)$$

IV. THE DATASET

The dataset employed in this work consists of ground-state dipole moments of 162 polar diatomic molecules, 139 of which have both information on the equilibrium bond length, R_e , and the harmonic vibrational frequency, ω_e . The dataset is presented in Table IV of the Appendix and it constitutes the most extensive dataset for dipole moments of diatomic molecules that we are aware of. Nevertheless, for more efficient scrutiny of our dataset's generality, we show in Fig. 2 the equilibrium bond length, R_e , versus the electric dipole moment of diatomic molecules. The density plots and the box plots show the distribution of R_e (right) and dipole moment, d , (top), respectively. The equilibrium bond length of the molecules is distributed between 0.9 and 3.9 Å with a median of around 1.5 Å, although most of the molecules show an equilibrium bond length between 1.2 and 3.2 Å. The dipole moment values in the dataset range from 0.0043 D to 11.69 D with a median of around 2.45 D, which shows the large variety of molecules included in the dataset.

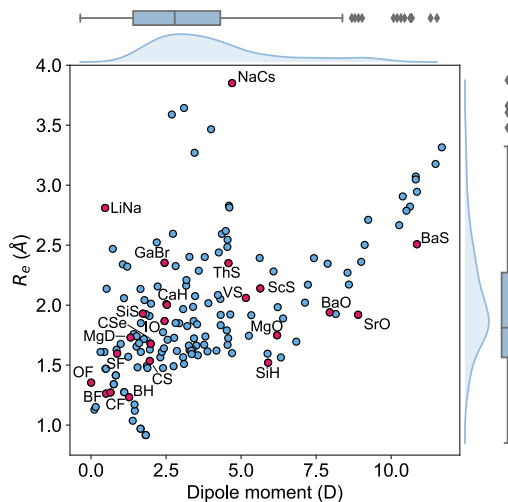


FIG. 2. The equilibrium bond length R_e versus the electric dipole moment of the molecules in the dataset. The blue filled circles are the molecules that can be learned by the GPR model in this work. The red filled circles indicate the molecules that can hardly be described by the GPR model in this work. These molecules are labeled by their chemical formula. The density in the right part and upper part of the figure shows the kernel density distribution of R_e and dipole moments, respectively. The box plot shows the minimum, the maximum, the sample median, and the first and third quarterlies of R_e (right) and dipole moments (top).

The dataset can also be categorized in terms of the type of atoms constituting the molecules, as it is shown in Fig. 1. In this figure, it is noticed that most of the molecules in the dataset present a highly ionic bond resulting from a transition metal and a nonmetal atom. The second most prominent group of molecules contains a halogen atom and an alkaline atom, which shows an ionic bond. The rest of the molecules exhibit a bond from partially ionic to highly ionic, which shows the diversity of the dataset.

V. RESULTS AND DISCUSSION

We have used a GPR approach to learn the diatomic molecules' dipole moment employing features coming from different atomic and molecular properties. The atomic properties considered are the electron affinity (EA), ionic potential (IP), electronegativity (χ) and polarizability (α) whereas the molecular properties are the reduced mass, μ , equilibrium bond length, R_e , and the harmonic vibrational frequency, ω_e . The atomic properties employed are related to the intrinsic chemical nature of the dipole moment due to the polarity of a molecular orbital in the molecular-orbital bond theory or to the ionic character of the molecular bond within the valence-bond theory.¹⁹ The GPR performance for different features is summarized in Table I, where we employ 118 out of the 139 molecules from the dataset having values for both R_e and ω_e .

After using different combinations of atomic and molecular properties, we find that the dipole moment of a di-

TABLE I. GPR Predictions on the ground-state dipole moments. g_i , p_i , EA_i , IP_i , χ_i , α_i are groups, periods, electron affinity, ionic potential, electronegativity and polarizability of the atom i , respectively. μ is the reduced mass of a molecule. For these results we employ 118 from the dataset out of the 139 molecules having values for both R_e and ω_e .

Feature	Test RMSE (D)	Test MAE (D)	Test r_E (%)
$(EA_1, EA_2, IP_1, IP_2, \sqrt{\mu R_e \omega_e^2})$	0.56 ± 0.02	0.43 ± 0.0004	4.8 ± 0.1
$(\chi_1, \chi_2, \sqrt{\mu R_e \omega_e^2})$	0.70 ± 0.05	0.52 ± 0.03	6.0 ± 0.4
$(EA_1, EA_2, IP_1, IP_2, \chi_1, \chi_2)$	0.86 ± 0.006	0.65 ± 0.02	7.4 ± 0.05
(EA_1, EA_2, IP_1, IP_2)	0.97 ± 0.05	0.74 ± 0.05	8.3 ± 0.4
$(EA_1, EA_2, IP_1, IP_2, R_e)$	1.04 ± 0.02	0.81 ± 0.04	9.1 ± 0.2
$(\chi^1, \chi_2, \alpha_1, \alpha_2)$	1.29 ± 0.004	1.01 ± 0.007	11.2 ± 0.04
(χ_1, χ_2)	1.35 ± 0.002	1.05 ± 0.009	11.7 ± 0.01
$(\sqrt{ \chi_1 - \chi_2 }, \bar{\alpha}, D_0^{-1})$	1.21 ± 0.03	0.96 ± 0.03	10.5 ± 0.3
$(p_1, p_2, g_1, g_2, R_e)$	1.25 ± 0.02	0.94 ± 0.04	10.8 ± 0.1

atomic molecule can be best learned by a GPR model using $(EA_1, EA_2, IP_1, IP_2, \sqrt{\mu R_e \omega_e^2})$ as the input features. The performance of this model is shown in Fig.3. The predicted values reproduce the true values very well with a small deviation that leads to a normalized error $r_E < 5\%$ (RMSE= 0.56 ± 0.02 D). We have also computed the learning curve of the cited GPR model, which gives an intuitive idea about the model’s learning and generalization performance concerning the size of the training set. The results are shown in the inset of Fig.3. The training RMSE and test RMSE are shown as a function of the number of training data points. The learning curve’s shade shows the variance of training/test RMSE, obtained for each point from a MC approach of 500 training/test splittings. The mean test error decreases with increasing training data. In particular, with 80 training data, the learning curve is almost converged, suggesting that this model can not benefit from more data of the same dataset. The error’s variance shows the ability of the model to be employed in different subgroups of molecules. In this case, the variance of test RMSE becomes smaller as the number of training data increases and converges to < 0.02 D with 60 training data.

In previous work, we have shown that R_e , ω_e , and the binding energy of a diatomic molecule can be learned through groups and periods of the constituent atoms as features⁹. However, the same features dramatically fail in learning the dipole moment. In particular, we find that the test errors are $RMSE = 1.25 \pm 0.02$ D and $r_E = 10.8 \pm 0.1\%$, respectively. In our view, this is an indication of the more intricate nature of the dipole moment compared to the spectroscopic constants of diatomic molecules.

In Ref.²⁵ it is shown that the dipole moment of diatomic alkali-alkaline earth molecules can be empirically calculated from the difference in the electronegativity of the constituent atoms $\sqrt{|\chi_1 - \chi_2|}$, the mean atomic polarizabilities $\bar{\alpha} = (\alpha_1 + \alpha_2)/2$ and the dissociation energy D_e . We have generalized this idea through a GPR model by using $(\sqrt{|\chi_1 - \chi_2|}, \bar{\alpha}, D_0^{-1})$ as features and applied it to the present dataset, despite the fact that alkaline earth-alkaline molecules are absent in the dataset. We have used the binding energy, D_0 , instead of the dissociation energy, as the former is tabulated more frequently. As a result, the normalized error is $r_E = 10.5 \pm 0.3\%$, which indicates that some of the physics behind the dipole moment

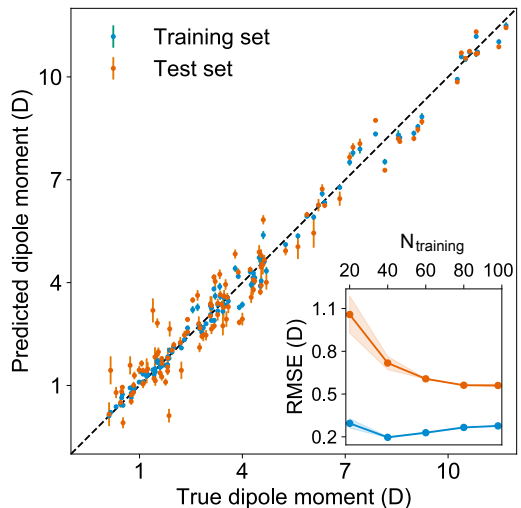


FIG. 3. The GPR predictions of the ground-state dipole moments. The values shown in this figure are the average of predictions from 1000 MC sampled training/test splittings²⁴. The test set contains 20 molecules, while the training set contains 98 molecules. The mean and standard deviation of the predictions are shown for each molecule when they are used as training data (shown in blue) and test data (shown in orange). The inset shows the learning curve, which shows the training and test RMSE of the model with respect to the number of training data. The shade in the learning curve shows the variance of training/test RMSE, obtained for each point from a MC approach of 500 training/test splittings.

function of alkali-alkaline earth molecules is applicable to any other molecule. This is an unexpected result that shows the underlying universality of the physics behind the dipole moment.

The outstanding performance of $(EA_1, EA_2, IP_1, IP_2, \sqrt{\mu R_e \omega_e^2})$ as the set of descriptors implies that the accepted picture in chemistry in which the difference of the electronegativity of the atoms within a molecule establishes the ionic character of the molecular bond^{17,19,26} is not sufficient to characterize the dipole moment of a molecule. When using the electron affinity and the atoms’ ionization potential as features, the performance improves by 25%. However, only

if $\sqrt{\mu R_e \omega_e^2}$ is included as a feature, the dipole moment is predicted with a RMSE below 0.7 D. Therefore, we find that it is essential to add $\sqrt{\mu R_e \omega_e^2}$ as a feature in describing the dipole moment of a diatomic molecule. It can be shown that this feature is related to the derivative of the electronic kinetic energy, $T(R)$, at the equilibrium bond length as²⁷

$$-\left. \frac{dT(R)}{dR} \right|_{R=R_e} = \mu R_e \omega_e^2, \quad (9)$$

which represents a force within the molecule. When equating this force to the pure electrostatic force, one obtains R_d and, through Eq.(4), it is then possible to define the ionic character as

$$IC = 100 \left(d \sqrt{\mu R_e \omega_e^2} \right)^{1/2}, \quad (10)$$

where the value of IC is given in percent. It is seen that IC does not directly depend upon the electronegativity differences of the atoms, contrary to the accepted picture in chemistry. The feature $\sqrt{\mu R_e \omega_e^2}$ was first introduced by Hou and Bernath^{10,11} as an empirical relationship, and we use this here to define the ionic character of a molecular bond.

Alternatively, the ionic character can be defined in terms of the electronegativity difference between the two atoms forming a molecule as

$$IC = 16|\chi_1 - \chi_2| + 3.5|\chi_1 - \chi_2|^2, \quad (11)$$

following Hannay and Smyth²⁶. Surprisingly, Eqs. 10 and 11 lead to different results for the ionic character of the molecules in the database, as shown in Fig. 4, where it is noticed that the distribution of the ionic character following Eq. 11 appears to be the complement to the one obtained from Eq. 10. Furthermore, the model of Hou and Bernath (Eq. 10) systematically leads to a larger ionic character than the model of Hannay and Smyth.

The GPR model with $(EA_1, EA_2, IP_1, IP_2, \sqrt{\mu R_e \omega_e^2})$ as input features shows several outliers. To see the importance of these outliers we have compared the distribution of the ionic character and dipole moment of the molecules in Fig. 4 (shown in grey) with the same magnitudes for the subset of 118 molecules that can be learned in this work (shown in blue). The ML-learned subset has similar overall distributions of dipole moments and ionic characters in comparison with the whole dataset. Therefore the outliers do not significantly modify the underlying distribution that the molecules follow.

In Table II, it is shown a classification of the outliers as a function of its molecular bond and constituent atoms. The effective atomic charges of these molecules are also calculated with a density functional theory (DFT) approach, which is shown in Table III utilizing different charge partitioning methods. The calculations are performed with the B3LYP functional²⁸ and def2-TZVP basis set²⁹⁻³¹, with the Gaussian 16 package³². We have noticed that for these outliers, the natural bond orbital (NBO) method gives larger effective atomic

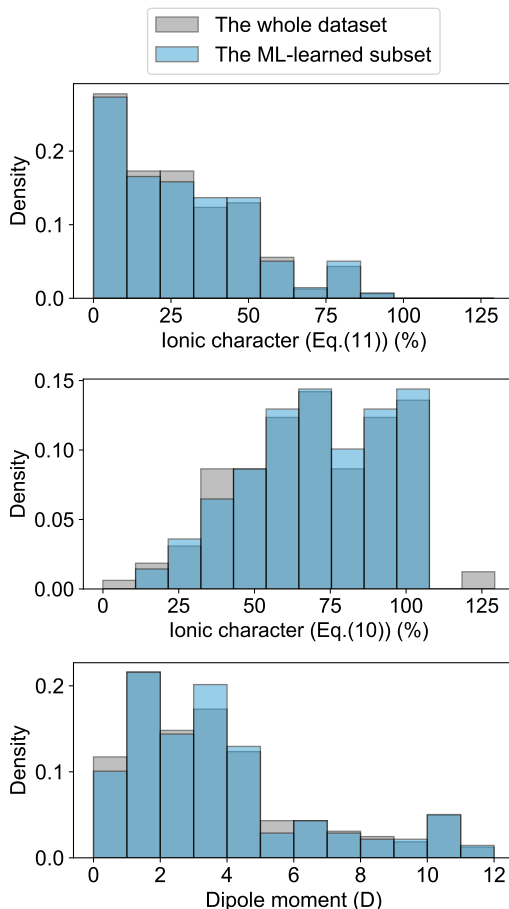


FIG. 4. Comparison of the histograms of ionic characters and dipole moments in the whole dataset (shown in grey) and the ML-learned subset of 118 molecules (shown in blue). Panel (a) and (b) show the ionic characters calculated from Eqs. (11) and (10), respectively. Panel (c) plots the histogram of the dipole moment of the molecules. It is worth noticing that the dark blue regions appear in regions where the grey and light-blue bars overlap.

charges compares to the Mulliken population. Furthermore, all the molecules showing a NBO charge larger than 1.0 are the ones showing an ionic character in virtue of Eq.10 above 100%. For the outliers within the van der Waals molecules, we find LiNa and NaCs. LiNa has the smallest R_e and dipole moment of the alkali metal molecules in this dataset, while NaCs has the largest R_e and dipole moment.

To understand the effect of different bonding types on the dipole moment, we plot in Fig. 5 the relationships between R_e and dipole moments for different kinds of molecules in the current dataset, where the outliers are shown in red circles. We observe that the relationships between R_e and dipole moments depend on the type of molecule under consideration. As shown in panel (a) of Fig. 5, R_e and dipole moments show linear relationship for metal-nonmetal molecules, in which the nonmetals atoms are from the same group in the periodic table. Similarly, linear behaviors have also been observed for the group IV/VI diatomic molecules in Ref.³³. For the oxygen halides shown in panel (b), R_e increases almost linearly

TABLE II. Outliers for learning the electric dipole moment of diatomic molecules. These molecules are labeled in Fig. 2 and classified with the types of constituent atoms and the molecular bonds.

Type of bond	Molecule
Nonmetal-nonmetal	IO, CS, SiS, CSe
Nonmetal-F	SF, BF, CF, OF
Metal-halogen	GaBr
Alkaline earth-nonmetal	BaO, SrO, MgO, SrS, BaS
Alkaline earth-H	MgD, CaH
Metalloid-H	BH, SiH
Transition metal-nonmetal	VS, ScS, ThS
van der Waals	LiNa, NaCs

TABLE III. The effective atomic charges of the outliers with different charge partitioning methods, calculated with the B3LYP functional²⁸ and def2-TZVP basis set^{29–31} with the Gaussian 16 package³².

Molecule	Mulliken	Hirschfeld	NBO
MgO	0.694	0.576	1.278
SrO	0.871	0.714	1.496
BaO	0.838	0.640	1.508
BaS	0.759	0.660	1.437
BF	0.099	0.073	0.549
CF	0.030	0.014	0.315
OF	0.017	0.012	0.063
SF	0.198	0.108	0.431
MgD	0.187	0.241	0.657
CaH	0.276	0.318	0.738
BH	-0.036	0.072	0.349
SiH	0.048	0.122	0.349
SiS	0.231	0.222	0.656
CS	-0.081	-0.087	-0.174
SeC	0.180	0.104	0.263
IO	0.412	0.214	0.625
GaBr	0.331	0.265	0.627
ScS	0.529	0.452	0.743
VS	0.425	0.247	0.343
CsNa	0.140	0.161	0.279
NaLi	-0.074	0.001	0.007

with the dipole moment. In panel (c), the molecules containing a transition metal and a nonmetal atom show a different trend of the equilibrium distance as a function of the dipole moment compared with the molecules formed by the main-group metal elements nonmetal atoms in panel (a). Within these molecules, the outliers are the ones with both the largest dipole moments and R_e in panel (c). Interestingly, we find that all the 4 alkaline earth-nonmetal molecules in the dataset are outliers, as shown in panel (d) of Fig. 5. Indeed, SrO, BaO and BaS have the largest atomic charges within the molecules in the dataset.

VI. CONCLUSION

In summary, we have shown that through a GPR model, the ground state dipole moments of diatomic molecules can be

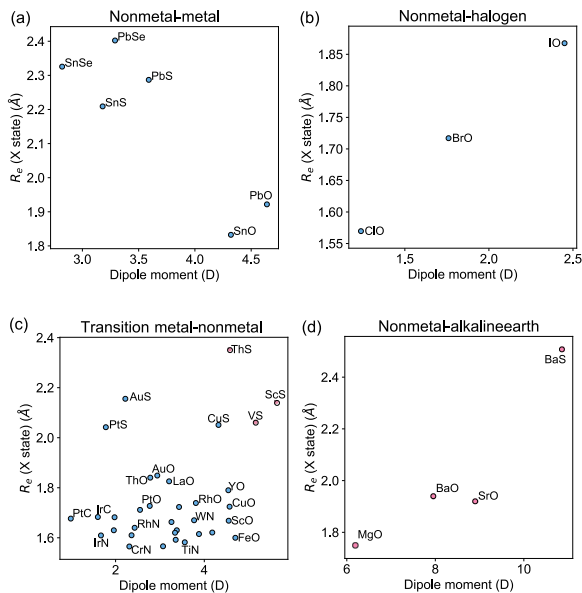


FIG. 5. The equilibrium bond lengths R_e as a function of dipole moments, classified by the type of the constituent atoms. The molecules that can be described by the GPR models from (EA₁, EA₂, IP₁, IP₂, $\sqrt{\mu R_e \omega_e^2}$) are shown in blue circles, while the outliers are shown in red circles.

related to spectroscopic constants, namely R_e and ω_e . More specifically, without any quantum chemistry calculation, the dipole moments of 118 molecules have been predicted with an error $\lesssim 5\%$ by using both atomic features, including electron affinity and ionic potential, and a combination of molecular spectroscopic constants, $\sqrt{\mu R_e \omega_e^2}$. In addition, we find that the difference in the electronegativity of the constituents atoms is not sufficient to describe the dipole moments of the diatomic molecules in stark contrast with what is generally assumed in general chemistry. Therefore, our data-driven approach shows that the nature of the dipole moment is more intricate than other spectroscopic constants, and it is clearly correlated with the very fundamental nature of the chemical bond. Finally, it is worth emphasizing that our findings have been possible thanks to the development of a complete and orthodox dataset.

ACKNOWLEDGMENTS

We thank Dr. Stefan Truppe for reading the manuscript and for useful comments and discussion regarding the nature of the electric dipole moment.

Appendix A: Details about GPR

The kernel function employed in this work, which gives the best CV scores, is the ration quadratic kernel²² defined by

$$k(x_i, x_j | \theta) = \sigma_f^2 \left(1 + \frac{r^2}{2\alpha\sigma_f^2} \right)^{-a}, \quad (\text{A1})$$

where σ_f is the length scale, and α is a scale-mixture parameter, r is the Euclidean distance between x_i and x_j defined as

$$r = \sqrt{(x_i - x_j)^T (x_i - x_j)}. \quad (\text{A2})$$

Appendix B: The dataset for dipole moment of diatomic molecules

The dataset is summarized in Table IV, which consists of dipole moments μ_0 of 162 polar diatomic molecules, 156 of which have information about equilibrium bond length R_e while 139 also have harmonic vibrational frequency ω_e . The references of the dipole moments are also listed in the table.

- ¹A. Kratzer, "Die ultraroten Rotationspektren der Halogenwasserstoffe," *Z. Phys.* **3**, 289 (1920).
- ²R. Mecke, "Zum Aufbau der Bandenspektren," *Z. Phys.* **32**, 823 (1925).
- ³P. M. Morse, "Diatomic molecules according to the wave mechanics. II. Vibrational levels," *Phys. Rev.* **34**, 57 (1929).
- ⁴R. M. Badger, "A relation between internuclear distances and bond force constants," *Journal of Chemical Physics* **2**, 128 (1933).
- ⁵C. D. Clark and J. L. Stoves, "A simple modification of Morse's rule," *Nature* **133**, 873 (1934).
- ⁶C. D. Clark, "XLIII. The relation between vibration frequency and nuclear separation for some simple non-hydride diatomic molecules," *The London, Edinburgh, and Dublin Philosophical Magazine and Journal of Science* **18**, 459–470 (1934).
- ⁷Y. P. Varshni, "Comparative study of potential energy functions for diatomic molecules," *Rev. Mod. Phys.* **29**, 664 (1957).
- ⁸Y. P. Varshni, "Correlation of molecular constants. II. Relation between force constant and equilibrium internuclear distance," *J. Chem. Phys.* **28**, 1081 (1958).
- ⁹X. Liu, G. Meijer, and J. Pérez-Ríos, "On the universality of spectroscopic constants of diatomic molecules," (2020), arXiv:2005.07913 [physics.chem-ph].
- ¹⁰S. Hou and P. F. Bernath, "Relationship between dipole moments and harmonic vibrational frequencies in diatomic molecules," *The Journal of Physical Chemistry A* **119**, 1435–1438 (2015).
- ¹¹S. Hou and P. F. Bernath, "Relationships between dipole moments of diatomic molecules," *Phys. Chem. Chem. Phys.* **17**, 4708–4713 (2015).
- ¹²G. R. Schleder, A. C. M. Padilha, C. M. Acosta, M. Costa, and A. Fazzio, "From DFT to machine learning: recent approaches to materials science—a review," *Journal of Physics: Materials* **2**, 032001 (2019).
- ¹³P. O. Dral, "Quantum chemistry in the age of machine learning," *The Journal of Physical Chemistry Letters* **11**, 2336–2347 (2020), pMID: 32125858, <https://doi.org/10.1021/acs.jpcllett.9b03664>.
- ¹⁴F. Noé, A. Tkatchenko, K.-R. Müller, and C. Clementi, "Machine learning for molecular simulation," *Annual Review of Physical Chemistry* **71**, 361–390 (2020), pMID: 32092281, <https://doi.org/10.1146/annurev-physchem-042018-052331>.
- ¹⁵J. Behler, "Perspective: Machine learning potentials for atomistic simulations," *The Journal of Chemical Physics* **145**, 170901 (2016), <https://doi.org/10.1063/1.4966192>.
- ¹⁶R. V. Krems, "Bayesian machine learning for quantum molecular dynamics," *Phys. Chem. Chem. Phys.* **21**, 13392–13410 (2019).
- ¹⁷L. Pauling, *The nature of the chemical bond and the structure of molecules and crystals : an introduction to modern structural chemistry (3rd ed.)* (Cornell University Press, Ithaca, N.Y., 1986).
- ¹⁸R. S. Mulliken, "Electronic structures of molecules xi. electroaffinity, molecular orbitals and dipole moments," *The Journal of Chemical Physics* **3**, 573–585 (1935), <https://doi.org/10.1063/1.1749731>.
- ¹⁹C. A. Coulson, *Valence* (Clarendon Press, Oxford, United Kingdom, 1952).
- ²⁰M. Klessinger, "Polarity of covalent bonds," *Angewandte Chemie International Edition in English* **9**, 500–512 (1970), <https://onlinelibrary.wiley.com/doi/pdf/10.1002/anie.197005001>.
- ²¹C. K. Williams and C. E. Rasmussen, *Gaussian processes for machine learning*, Vol. 2 (MIT press Cambridge, MA, 2006).
- ²²MATLAB, *9.7.0 (R2019b)* (The MathWorks Inc., Natick, Massachusetts, 2019).
- ²³S. Raschka, "Model evaluation, model selection, and algorithm selection in machine learning," arXiv preprint arXiv:1811.12808 (2018).
- ²⁴X. Liu, G. Meijer, and J. Pérez-Ríos, To be published.
- ²⁵J. V. Pototschnig, A. W. Hauser, and W. E. Ernst, "Electric dipole moments and chemical bonding of diatomic alkali–alkaline earth molecules," *Physical Chemistry Chemical Physics* **18**, 5964–5973 (2016).
- ²⁶N. B. Hannay and C. P. Smyth, "The dipole moment of hydrogen fluoride and the ionic character of bonds," *Journal of the American Chemical Society* **68**, 171–173 (1946), <https://doi.org/10.1021/ja01206a003>.
- ²⁷R. F. Borkman and R. G. Parr, "Toward an understanding of potential-energy functions for diatomic molecules," *The Journal of Chemical Physics* **48**, 1116–1126 (1968), <https://doi.org/10.1063/1.1668772>.
- ²⁸P. J. Stephens, F. Devlin, C. Chabalowski, and M. J. Frisch, "Ab initio calculation of vibrational absorption and circular dichroism spectra using density functional force fields," *The Journal of physical chemistry* **98**, 11623–11627 (1994).
- ²⁹M. Kaupp, P. v. R. Schleyer, H. Stoll, and H. Preuss, "Pseudopotential approaches to Ca, Sr, and Ba hydrides. Why are some alkaline earth MX₂ compounds bent?" *The Journal of chemical physics* **94**, 1360–1366 (1991).
- ³⁰T. Leininger, A. Nicklass, W. Küchle, H. Stoll, M. Dolg, and A. Bergner, "The accuracy of the pseudopotential approximation: Non-frozen-core effects for spectroscopic constants of alkali fluorides XF (X = K, Rb, Cs)," *Chemical physics letters* **255**, 274–280 (1996).
- ³¹F. Weigend and R. Ahlrichs, "Balanced basis sets of split valence, triple zeta valence and quadruple zeta valence quality for H to Rn: Design and assessment of accuracy," *Physical Chemistry Chemical Physics* **7**, 3297–3305 (2005).
- ³²M. J. Frisch, G. W. Trucks, H. B. Schlegel, G. E. Scuseria, M. A. Robb, J. R. Cheeseman, G. Scalmani, V. Barone, G. A. Petersson, H. Nakatsuji, X. Li, M. Caricato, A. V. Marenich, J. Bloino, B. G. Janesko, R. Gomperts, B. Mennucci, H. P. Hratchian, J. V. Ortiz, A. F. Izmaylov, J. L. Sonnenberg, D. Williams-Young, F. Ding, F. Lipparini, F. Egidi, J. Goings, B. Peng, A. Petrone, T. Henderson, D. Ranasinghe, V. G. Zakrzewski, J. Gao, N. Rega, G. Zheng, W. Liang, M. Hada, M. Ehara, K. Toyota, R. Fukuda, J. Hasegawa, M. Ishida, T. Nakajima, Y. Honda, O. Kitao, H. Nakai, T. Vreven, K. Throssell, J. A. Montgomery, Jr., J. E. Peralta, F. Ogliaro, M. J. Bearpark, J. J. Heyd, E. N. Brothers, K. N. Kudin, V. N. Staroverov, T. A. Keith, R. Kobayashi, J. Normand, K. Raghavachari, A. P. Rendell, J. C. Burant, S. S. Iyengar, J. Tomasi, M. Cossi, J. M. Millam, M. Klene, C. Adamo, R. Cammi, J. W. Ochterski, R. L. Martin, K. Morokuma, O. Farkas, J. B. Foresman, and D. J. Fox, "Gaussian 16 Revision C.01," (2016), Gaussian Inc. Wallingford CT.
- ³³J. Hoelt, F. Lovas, E. Tiemann, and T. Törring, "Dipole moments and hyperfine structure of the group IV/VI diatomic molecules," *The Journal of Chemical Physics* **53**, 2736–2743 (1970).
- ³⁴K. P. Huber and G. Herzberg, *Molecular Spectra and Molecular Structure* (Springer-Verlag, Berlin, Germany, 1979).
- ³⁵B. M. Smirnov, *Reference Data on Atomic Physics and Atomic Processes* (Springer-Verlag, Berlin, Germany, 2008).
- ³⁶W. M. Haynes, *CRC handbook of chemistry and physics* (CRC press, 2014).
- ³⁷J. Hoelt, F. Lovas, E. Tiemann, and T. Törring, "Elektrisches Dipolmoment von GeSe, GeTe, PbSe und PbTe," *Zeitschrift für Naturforschung A* **25**, 539 (1970).

TABLE IV. The dipole moments, d , equilibrium bond length, R_e , and harmonic vibrational frequency, ω_e , employed in this work. The references to the dipole moments are also listed in the table. R_e and ω_e are taken from Ref. ^{34,35} or the same reference of the dipole moment of the corresponding molecules, except as indicated.

Molecule	d (D)	R_e (Å)	ω_e (cm ⁻¹)	Ref.	Molecule	d (D)	R_e (Å)	ω_e (cm ⁻¹)	Ref.	Molecule	d (D)	R_e (Å)	ω_e (cm ⁻¹)	Ref.
AgBr	5.62	2.393	247.7	³⁶	GeTe	1.06	2.34	323.9	³⁷	PbSe	3.29	2.402	277.6	³⁷
AgCl	6.08	2.281	343.5	³⁶	DBr	0.823	1.415	1884.8	³⁸	PbTe	2.73	2.595	212	³⁷
AgF	6.22	1.983	513.5	³⁹	HBr	0.8272	1.414	2649	³⁶	PN	2.7514	1.491	1337.2	⁴⁰
AgH	2.86	1.618	1759.9	⁴¹	DF	1.819	0.917	2998.2	³⁸	PO	1.88	1.476	1233.3	⁴²
AgI	4.55	2.545	206.5	³⁶	HF	1.826526	0.917	4138.3	⁴³	PtC	0.99	1.677	1051.1	⁴⁴
AlF	1.515	1.654	802.3	⁴⁵	HfF	1.66	1.85		⁴⁶	PtF	3.42	1.868		⁴⁷
AuF	4.32	1.918	539.4 ^a	⁴⁸	HfO	3.431	1.723	974.1	⁴⁹	PtN	1.977	1.682		⁵⁰
AuO	2.94	1.849	624.59 ^b	⁵¹	HI	0.448	1.609	2309	³⁶	PtO	2.77	1.727	851.1	⁴⁴
AuS	2.22	2.156	410.19 ^c	⁵¹	IBr	0.726	2.469	268.6	³⁶	PtS	1.78	2.042		⁴⁴
BaF	3.17	2.163	468.9	⁵²	ICl	1.207	2.321	384.3	⁵³	RbBr	10.86	2.945	169.5	⁵⁴
BaO	7.955	1.94	669.8	⁵⁵	ID	0.316	1.609	1639.7	⁵⁶	RbCl	10.51	2.787	228	⁵⁷
BaS	10.86	2.507	379.4	⁵⁸	IF	1.948	1.91	610.2	³⁶	RbF	8.5465	2.27	376	⁵⁷
BF	0.5	1.263	1402.1	⁵⁹	InCl	3.79	2.401	317.4	³⁶	RbI	11.48	3.177	138.5	⁵⁴
BH	1.27	1.232	2366.9	⁶⁰	InF	3.4	1.985	535.4	⁶¹	ReN	1.96	0.61		⁶²
BrCl	0.519	2.136	444.3	³⁶	IO	2.45	1.868	681.5	⁶³	RhN	2.43	1.64		⁶⁴
BrF	1.422	1.759	670.8	³⁶	IrC	1.6	1.683	1060.1	⁶⁵	RhO	3.81	1.739		⁶⁶
BrO	1.76	1.717	778.7	³⁸	IrF	2.82	1.851		⁶⁷	RuF	5.34	1.916		⁶⁸
CaBr	4.36	2.594	285.3 ^d	⁶⁹	IrN	1.67	1.609		⁶⁵	ScO	4.55	1.668	965	⁷⁰
CaCl	4.257	2.439	367.5	⁶⁹	KBr	10.6281	2.821	213	⁷¹	ScS	5.64	2.139	565.2	⁷²
CaD	2.51	2.01		⁷³	KCl	10.2688	2.667	281	⁵⁷	SD	0.7571	1.341	1885.5	⁷⁴
CaF	3.07	1.967	581.1	⁷⁵	KF	8.59255	2.171	428	⁷¹	SeF	1.52	1.741	757	⁶³
CaH	2.53	2.003	1298.3	⁷³	KI	10.82	3.048	186.5	⁵⁴	SeD	0.48	1.47	1708	³⁸
CaI	4.5968	2.829	238.7	⁷⁶	LaO	3.207	1.826	812.8	⁴⁹	SeH	0.5	1.47	2400	³⁸
CF	0.65	1.272	1308.1	⁶³	LiBr	7.2262	2.17	563.2	⁷⁷	SF	0.87	1.596	837.6	⁶³
CH	1.46	1.12	2858.5	³⁶	LiCl	7.1289	2.021	643.3	⁵⁷	SH	0.758	1.341	2711.6	⁷⁸
CID	1.1033	1.275	2145.2	⁷⁹	LiF	6.32736	1.564	910.3	⁵⁷	SiH	5.9	1.52	2041.8	³⁸
CIF	0.85	1.628	786.2	⁸⁰	LiH	5.882	1.596	1405.7	⁸¹	SiO	3.0982	1.51	1241.6	⁸²
CIH	1.1085	1.275	2990.9	⁷⁹	LiI	7.4285	2.392	498.2	⁸³	SiS	1.73	1.73	749.6	⁸⁴
CIO	1.239	1.57	853.8	⁸⁵	LiK	3.45	3.27	207	³⁶	SiSe	1.1	2.058	580	³³
CN	1.45	1.172	2068.6	⁸⁶	LiNa	0.47	2.81	256.8	⁸⁷	SnO	4.32	1.833	814.6	³³
CO	0.112	1.128	2169.8	⁵⁶	LiO	6.84	1.695	851.5	³⁶	SnS	3.18	2.209	487.3	³³
CoF	2.82			⁸⁸	LiRb	4.0	3.466	195.2	³⁶	SnSe	2.82	2.326	331.2	³³
CoH	1.88			⁸⁸	MgD	1.318	1.73	1077.9	⁸⁹	SnTe	2.19	2.523	259	³³
CoO	4.18	1.621		⁹⁰	MgO	6.2	1.749	785.1	³⁶	SO	1.55	1.481	1149.2	⁹¹
CrD	3.51	1.663	1182	⁹²	MoC	6.07			⁹³	SrF	3.4676	2.075	502.4	⁹⁴
CrN	2.31	1.5652 ^e	854.0 ^f	⁹⁵	MoN	3.38	1.63		⁹⁶	SrO	8.9	1.92	653.5	³⁸
CrO	3.88	1.615	898.4	⁹⁷	NaBr	9.1183	2.502	302.1	⁵⁷	ThO	3.534	1.84	895.8	⁹⁸
CS	1.958	1.535	1285.1	⁹⁹	NaCl	9.002	2.361	366	⁵⁷	ThS	4.58	2.35	477 ^g	¹⁰⁰
CsBr	10.82	3.072	149.7	⁵⁴	NaCs	4.7	3.851	98.9	³⁸	TiH	2.455			¹⁰¹
CsCl	10.387	2.906	214.2	⁵⁷	NaF	8.1558	1.926	536	¹⁰²	TiO	3.34	1.62	1009	¹⁰³
CSe	1.99	1.676	1035.4	¹⁰⁴	NaH	6.4	1.889	1176	¹⁰⁵	TiN	3.56	1.582 ^h	1039 ⁱ	¹⁰⁶
CsF	7.8839	2.345	352.6	⁵⁷	NaI	9.2357	2.711	258	⁵⁷	TIBr	4.49	2.618	192.1	³⁸
CsI	11.69	3.315	119.2	⁵⁴	NaK	2.693	3.589	124.1	³⁶	TiCl	4.5429	2.485	283.8	³³
CuF	5.26	1.745	622.7	¹⁰⁷	NaRb	3.1	3.644	106.9	³⁶	TIF	4.2282	2.084	477.3	¹⁰⁸
CuO	4.57	1.724	640.2	¹⁰⁹	NbN	3.26	1.663		¹¹⁰	TII	4.61	2.814	143	³⁶
CuS	4.31	2.051	415	¹¹¹	NH	1.39	1.036	3282.3	³⁶	VN	3.07	1.566 ^j	1033 ^k	⁹⁵
FeC	2.36	1.61		¹¹²	NiH	2.4	1.476	1926.6	¹¹³	VO	3.355	1.592 ^l	1011.3	¹¹⁴
FeH	2.63			¹¹⁵	NO	0.157	1.151	1904.2	¹¹⁶	VS	5.16	2.06		¹¹⁷
FeO	4.7	1.6	970	¹¹⁸	NS	1.86	1.494	1218.7	⁶³	WC	3.9			¹¹⁹
GaF	2.4	1.774	622.2	³⁸	OD	1.653	0.97	2720.2	³⁸	WN	3.77	1.67 ^m		⁶²
GaBr	2.45	2.352	263	³³	OF	0.0043	1.354	1028.7	³⁶	YbF	3.91	2.016	501.9	¹²⁰
GeO	3.2824	1.625	985.5	⁸²	OH	1.6498	0.97	3737.8	¹²¹	YF	1.82	1.926	631.3	¹²²
GeS	2	2.012	575.8	³³	PbO	4.64	1.922	721	¹²³	YO	4.524	1.79	861	⁴⁹
GeSe	1.648	2.135	408.7	³⁷	PbS	3.59	2.287	429.4	¹²³	ZrO	2.551	1.712	969.8	⁴⁹

^a From Ref.¹²⁴.^b From Ref.¹²⁵.^c From Ref.¹²⁶.^d From Ref.¹²⁷.^e From Ref.¹²⁸.^f From Ref.¹²⁹.^g From Ref.¹³⁰.^h From Ref.¹³¹.ⁱ From Ref.¹³².^j From Ref.¹³³.^k From Ref.¹³⁴.^l From Ref.¹³⁵.^m From Ref.¹³⁶.

- ³⁸A. A. Radzig and B. M. Smirnov, *Reference data on atoms, molecules, and ions*, Vol. 31 (Springer Science & Business Media, 2012).
- ³⁹J. Hoefl, F. Lovas, E. Tiemann, and T. Törring, "The rotational spectra and dipole moments of AgF and CuF by microwave absorption," *Zeitschrift für Naturforschung A* **25**, 35–39 (1970).
- ⁴⁰F. Wyse, E. Manson, and W. Gordy, "Millimeter wave rotational spectrum and molecular constants of $^{31}\text{P}^{14}\text{N}$," *The Journal of Chemical Physics* **57**, 1106–1108 (1972).
- ⁴¹A. J. Sadlej and M. Urban, "Mutual dependence of relativistic and electron correlation contributions to molecular properties: the dipole moment of AgH," *Chemical physics letters* **176**, 293–302 (1991).
- ⁴²H. Kanata, S. Yamamoto, and S. Saito, "The dipole moment of the PO radical determined by microwave spectroscopy," *Journal of Molecular Spectroscopy* **131**, 89–95 (1988).
- ⁴³J. Muentner and W. Klemperer, "Hyperfine structure constants of HF and DF," *The Journal of Chemical Physics* **52**, 6033–6037 (1970).
- ⁴⁴T. Steimle, K. Jung, and B.-Z. Li, "The permanent electric dipole moment of PtO, PtS, PtN, and PtC," *The Journal of chemical physics* **103**, 1767–1772 (1995).
- ⁴⁵S. Truppe, S. Marx, S. Kray, M. Doppelbauer, S. Hofsäss, H. C. Schewe, N. Walter, J. Pérez-Ríos, B. G. Sartakov, and G. Meijer, "Spectroscopic characterization of aluminum monofluoride with relevance to laser cooling and trapping," *Phys. Rev. A* **100**, 052513 (2019).
- ⁴⁶A. Le, T. C. Steimle, L. Skripnikov, and A. V. Titov, "The molecular frame electric dipole moment and hyperfine interactions in hafnium fluoride, HfF," *The Journal of chemical physics* **138**, 124313 (2013).
- ⁴⁷C. Qin, R. Zhang, F. Wang, and T. C. Steimle, "The permanent electric dipole moment and hyperfine interactions in platinum monofluoride, PtF," *The Journal of chemical physics* **137**, 054309 (2012).
- ⁴⁸T. C. Steimle, R. Zhang, C. Qin, and T. D. Varberg, "Molecular-beam optical Stark and Zeeman study of the $[17.8] 0^+ - X^1\Sigma^+(0, 0)$ band system of AuF," *The Journal of Physical Chemistry A* **117**, 11737–11744 (2013).
- ⁴⁹R. Suenram, F. Lovas, G. Fraser, and K. Matsumura, "Pulsed-nozzle fourier-transform microwave spectroscopy of laser-vaporized metal oxides: Rotational spectra and electric dipole moments of YO, LaO, ZrO, and HfO," *The Journal of chemical physics* **92**, 4724–4733 (1990).
- ⁵⁰K. Jung, T. Steimle, D. Dai, and K. Balasubramanian, "Experimental determination of dipole moments, hyperfine interactions, and *ab initio* predictions for PtN," *The Journal of chemical physics* **102**, 643–652 (1995).
- ⁵¹R. Zhang, Y. Yu, T. C. Steimle, and L. Cheng, "The electric dipole moments in the ground states of gold oxide, AuO, and gold sulfide, AuS," *The Journal of chemical physics* **146**, 064307 (2017).
- ⁵²W. Ernst, J. Kändler, and T. Törring, "Hyperfine structure and electric dipole moment of BaF $X^2\Sigma^+$," *The Journal of chemical physics* **84**, 4769–4773 (1986).
- ⁵³A. Durand, J. Loison, and J. Vigué, "Spectroscopy of pendular states: Determination of the electric dipole moment of ICl in the $X^1\Sigma^+(v''=0)$ and $A^3\Pi_1(v''=6-29)$ levels," *The Journal of chemical physics* **106**, 477–484 (1997).
- ⁵⁴T. Story Jr and A. Hebert, "Dipole moments of KI, RbBr, RbI, CsBr, and CsI by the electric deflection method," *The Journal of Chemical Physics* **64**, 855–858 (1976).
- ⁵⁵L. Wharton, M. Kaufman, and W. Klemperer, "Electric resonance spectrum and dipole moment of BaO," *The Journal of Chemical Physics* **37**, 621–626 (1962).
- ⁵⁶C. A. Burrus, "Stark effect from 1.1 to 2.6 millimeters wavelength: PH₃, PD₃, DI, and CO," *The Journal of Chemical Physics* **28**, 427–429 (1958).
- ⁵⁷A. Hebert, F. Lovas, C. Melendres, C. Hollowell, T. Story Jr, and K. Street Jr, "Dipole moments of some alkali halide molecules by the molecular beam electric resonance method," *The Journal of Chemical Physics* **48**, 2824–2825 (1968).
- ⁵⁸C. Melendres, A. Hebert, and K. Street Jr, "Radio-frequency Stark spectra and dipole moment of BaS," *The Journal of Chemical Physics* **51**, 855–856 (1969).
- ⁵⁹F. J. Lovas and D. R. Johnson, "Microwave spectrum of BF," *The Journal of Chemical Physics* **55**, 41–44 (1971).
- ⁶⁰R. Thomson and F. Dalby, "An experimental determination of the dipole moments of the X ($^1\Sigma$) and A ($^1\Pi$) states of the BH molecule," *Canadian Journal of Physics* **47**, 1155–1158 (1969).
- ⁶¹J. Hoefl, F. Lovas, E. Tiemann, and T. Törring, "Microwave absorption spectra of AlF, GaF, InF, and TlF," *Zeitschrift für Naturforschung A* **25**, 1029–1035 (1970).
- ⁶²T. C. Steimle and W. L. Virgo, "The permanent electric dipole moments of WN and ReN and nuclear quadrupole interaction in ReN," *The Journal of chemical physics* **121**, 12411–12420 (2004).
- ⁶³C. Byfleet, A. Carrington, and D. Russell, "Electric dipole moments of open-shell diatomic molecules," *Molecular Physics* **20**, 271–277 (1971).
- ⁶⁴T. Ma, J. Gengler, Z. Wang, H. Wang, and T. C. Steimle, "Molecular beam optical Stark study of rhodium mononitride," *The Journal of chemical physics* **126**, 244312 (2007).
- ⁶⁵A. J. Marr, M. Flores, and T. Steimle, "The optical and optical/Stark spectrum of iridium monocarbide and mononitride," *The Journal of chemical physics* **104**, 8183–8196 (1996).
- ⁶⁶J. Gengler, T. Ma, A. G. Adam, and T. C. Steimle, "A molecular beam optical Stark study of the $[15.8]$ and $[16.0] ^2\Pi_{1/2} - X^4\Sigma^-(0, 0)$ band systems of rhodium monoxide, RhO," *The Journal of chemical physics* **126**, 134304 (2007).
- ⁶⁷X. Zhuang, T. C. Steimle, and C. Linton, "The electric dipole moment of iridium monofluoride, IrF," *The Journal of chemical physics* **133**, 164310 (2010).
- ⁶⁸T. C. Steimle, W. L. Virgo, and T. Ma, "The permanent electric dipole moment and hyperfine interaction in ruthenium monofluoride (RuF)," *The Journal of chemical physics* **124**, 024309 (2006).
- ⁶⁹T. Törring, W. Ernst, and S. Kindt, "Dipole moments and potential energies of the alkaline earth monohalides from an ionic model," *The Journal of chemical physics* **81**, 4614–4619 (1984).
- ⁷⁰J. Shirley, C. Scurlock, and T. Steimle, "Molecular-beam optical Stark spectroscopy of ScO," *The Journal of chemical physics* **93**, 1568–1575 (1990).
- ⁷¹R. Van Wachem, F. De Leeuw, and A. Dymanus, "Dipole moments of KF and KBr measured by the molecular-beam electric-resonance method," *The Journal of Chemical Physics* **47**, 2256–2258 (1967).
- ⁷²T. Steimle, A. Marr, and D. Goodridge, "Dipole moments and hyperfine interactions in scandium monosulfide, ScS," *The Journal of chemical physics* **107**, 10406–10414 (1997).
- ⁷³J. Chen and T. C. Steimle, "The permanent electric dipole moment of calcium monodeuteride," *The Journal of chemical physics* **128**, 144312 (2008).
- ⁷⁴W. Meerts and A. Dymanus, "A molecular beam electric resonance study of the hyperfine Λ doubling spectrum of OH, OD, SH, and SD," *Canadian Journal of Physics* **53**, 2123–2141 (1975).
- ⁷⁵W. Childs, L. Goodman, U. Nielsen, and V. Pfeufer, "Electric-dipole moment of CaF ($X^2\Sigma^+$) by molecular beam, laser-rf, double-resonance study of Stark splittings," *The Journal of chemical physics* **80**, 2283–2287 (1984).
- ⁷⁶W. Ernst, J. Kändler, J. Lüdtke, and T. Törring, "Precise measurement of the ground state dipole moment of CaI," *The Journal of chemical physics* **83**, 2744–2747 (1985).
- ⁷⁷A. Hebert, F. Breivogel Jr, and K. Street Jr, "Radio-frequency and microwave spectra of LiBr by the molecular-beam electric-resonance method," *The Journal of Chemical Physics* **41**, 2368–2376 (1964).
- ⁷⁸W. Meerts and A. Dymanus, "The hyperfine lambda-doubling spectrum of sulfur hydride in the $^2\Pi_{3/2}$ state," *The Astrophysical Journal* **187**, L45 (1974).
- ⁷⁹E. W. Kaiser, "Dipole moment and hyperfine parameters of H³⁵Cl and D³⁵Cl," *The Journal of Chemical Physics* **53**, 1686–1703 (1970).
- ⁸⁰B. Fabricant and J. Muentner, "Molecular beam Zeeman effect and dipole moment sign of ClF," *The Journal of Chemical Physics* **66**, 5274–5277 (1977).
- ⁸¹L. Wharton, L. P. Gold, and W. Klemperer, "Dipole moment of lithium hydride," *The Journal of Chemical Physics* **33**, 1255–1255 (1960).
- ⁸²J. W. Raymonda, J. S. Muentner, and W. A. Klemperer, "Electric dipole moment of SiO and GeO," *The Journal of Chemical Physics* **52**, 3458–3461 (1970).
- ⁸³F. Breivogel Jr, A. Hebert, and K. Street Jr, "Radio-frequency and microwave spectra of $^6\text{Li}^{127}\text{I}$ by the molecular-beam electric-resonance method," *The Journal of Chemical Physics* **42**, 1555–1558 (1965).
- ⁸⁴J. Lovas, F. Hoefl, E. Tiemann, and T. Törring, "Elektrisches Dipolmoment und Mikrowellen-rotationsspektrum von SiS," *Zeitschrift für Natur-*

- forschung A **24**, 1422 (1969).
- ⁸⁵T. Amano, S. Saito, E. Hirota, Y. Morino, D. Johnson, and F. Powell, "Microwave spectrum of the ClO radical," *Journal of Molecular Spectroscopy* **30**, 275–289 (1969).
- ⁸⁶R. Thomson and F. Dalby, "Experimental determination of the dipole moments of the X ($^2\Sigma^+$) and B ($^2\Sigma^+$) states of the CN molecule," *Canadian Journal of Physics* **46**, 2815–2819 (1968).
- ⁸⁷P. Dagdigian, J. Graff, and L. Wharton, "Stark effect of NaLi X $^1\Sigma^+$," *The Journal of Chemical Physics* **55**, 4980–4982 (1971).
- ⁸⁸H. Wang, X. Zhuang, and T. C. Steimle, "The permanent electric dipole moments of cobalt monofluoride, CoF, and monohydride, CoH," *The Journal of chemical physics* **131**, 114315 (2009).
- ⁸⁹T. C. Steimle, R. Zhang, and H. Wang, "The electric dipole moment of magnesium deuteride, MgD," *The Journal of chemical physics* **140**, 224308 (2014).
- ⁹⁰X. Zhuang and T. C. Steimle, "The electric dipole moment of cobalt monoxide, CoO," *The Journal of chemical physics* **140**, 124301 (2014).
- ⁹¹F. Powell and D. R. Lide Jr, "Microwave spectrum of the SO radical," *The Journal of Chemical Physics* **41**, 1413–1419 (1964).
- ⁹²J. Chen, T. C. Steimle, and A. J. Merer, "The permanent electric dipole moment of chromium monodeuteride, CrD," *The Journal of chemical physics* **127**, 204307 (2007).
- ⁹³H. Wang, W. L. Virgo, J. Chen, and T. C. Steimle, "Permanent electric dipole moment of molybdenum carbide," *The Journal of chemical physics* **127**, 124302 (2007).
- ⁹⁴W. Ernst, J. Kändler, S. Kindt, and T. Törring, "Electric dipole moment of SrF X $^2\Sigma^+$ from high-precision Stark effect measurements," *Chemical physics letters* **113**, 351–354 (1985).
- ⁹⁵T. C. Steimle, J. S. Robinson, and D. Goodridge, "The permanent electric dipole moments of chromium and vanadium mononitride: CrN and VN," *The Journal of chemical physics* **110**, 881–889 (1999).
- ⁹⁶D. Fletcher, K. Jung, and T. Steimle, "Molecular beam optical Stark spectroscopy of MoN," *The Journal of chemical physics* **99**, 901–905 (1993).
- ⁹⁷T. C. Steimle, D. F. Nachman, J. E. Shirley, C. W. Bauschlicher Jr, and S. R. Langhoff, "The permanent electric dipole moment of chromium monoxide," *The Journal of chemical physics* **91**, 2049–2053 (1989).
- ⁹⁸F. Wang, A. Le, T. C. Steimle, and M. C. Heaven, "Communication: The permanent electric dipole moment of thorium monoxide, ThO," (2011).
- ⁹⁹G. Winnewisser and R. L. Cook, "The dipole moment of carbon monosulfide," *Journal of Molecular Spectroscopy* **28**, 266–268 (1968).
- ¹⁰⁰A. Le, M. C. Heaven, and T. C. Steimle, "The permanent electric dipole moment of thorium sulfide, ThS," *The Journal of chemical physics* **140**, 024307 (2014).
- ¹⁰¹T. Steimle, J. Shirley, B. Simard, M. Vasseur, and P. Hackett, "A laser spectroscopic study of gas-phase TiH," *The Journal of chemical physics* **95**, 7179–7182 (1991).
- ¹⁰²C. Hollowell, A. Hebert, and K. Street Jr, "Radio-frequency and microwave spectra of NaF by the molecular-beam electric-resonance method," *The Journal of Chemical Physics* **41**, 3540–3545 (1964).
- ¹⁰³T. C. Steimle and W. Virgo, "The permanent electric dipole moments of the X $^3\Delta$, E $^3\Pi$, A $^3\Phi$ and B $^3\Pi$ states of titanium monoxide, TiO," *Chemical physics letters* **381**, 30–36 (2003).
- ¹⁰⁴J. McGurk, H. Tigelaar, S. Rock, C. Norris, and W. Flygare, "Detection, assignment of the microwave spectrum and the molecular Stark and Zeeman effects in CSe, and the Zeeman effect and sign of the dipole moment in CS," *The Journal of Chemical Physics* **58**, 1420–1424 (1973).
- ¹⁰⁵P. J. Dagdigian, "Ground state dipole moment of NaH," *The Journal of Chemical Physics* **71**, 2328–2329 (1979).
- ¹⁰⁶B. Simard, H. Niki, and P. Hackett, "The permanent dipole moment of TiN and the nuclear magnetic hyperfine structure in its X $^2\Sigma^+$ and a $^2\Pi$ electronic states," *The Journal of Chemical Physics* (1990).
- ¹⁰⁷F. Wang and T. C. Steimle, "Hyperfine interaction and Stark effect in the b $^3\Pi-X^1\Sigma^+(0, 0)$ band of copper monofluoride, CuF," *The Journal of chemical physics* **132**, 054301 (2010).
- ¹⁰⁸R. v. Boeckh, G. Gräff, and R. Ley, "Die Abhängigkeit innerer und äußerer Wechselwirkungen des TIF-Moleküls von der Schwingung, Rotation und Isotopie," *Zeitschrift für Physik* **179**, 285–313 (1964).
- ¹⁰⁹X. Zhuang, S. E. Frey, and T. C. Steimle, "Permanent electric dipole moment of copper monoxide, CuO," *The Journal of chemical physics* **132**, 234312 (2010).
- ¹¹⁰D. Fletcher, D. Dai, T. Steimle, and K. Balasubramanian, "The permanent electric dipole moment of NbN," *The Journal of chemical physics* **99**, 9324–9325 (1993).
- ¹¹¹T. C. Steimle, W.-L. Chang, D. F. Nachman, and J. M. Brown, "Electronic properties of CuS: Experimental determination of the magnetic hyperfine interactions and permanent electric dipole moment," *The Journal of chemical physics* **89**, 7172–7179 (1988).
- ¹¹²T. C. Steimle, W. L. Virgo, and D. A. Hostutler, "The permanent electric dipole moments of iron monocarbide, FeC," *The Journal of chemical physics* **117**, 1511–1516 (2002).
- ¹¹³J. A. Gray, S. F. Rice, and R. Field, "The electric dipole moment of NiH X $^2\Delta_{5/2}$ and B $^2\Delta_{5/2}$," *The Journal of Chemical Physics* **82**, 4717–4718 (1985).
- ¹¹⁴R. Suenram, G. T. Fraser, F. J. Lovas, and C. Gillies, "Microwave spectra and electric dipole moments of X $^4\Sigma_{12}^{-1}$ VO and NbO," *Journal of Molecular Spectroscopy* **148**, 114–122 (1991).
- ¹¹⁵T. C. Steimle, J. Chen, J. J. Harrison, and J. M. Brown, "A molecular-beam optical Stark study of lines in the (1, 0) band of the F $^4\Delta_{7/2}-X^4\Delta_{7/2}$ transition of iron monohydride, FeH," *The Journal of chemical physics* **124**, 184307 (2006).
- ¹¹⁶A. Hoy, J. Johns, and A. McKellar, "Stark spectroscopy with the CO laser: dipole moments, hyperfine structure, and level crossing effects in the fundamental band of NO," *Canadian Journal of Physics* **53**, 2029–2039 (1975).
- ¹¹⁷X. Zhuang and T. C. Steimle, "The permanent electric dipole moment of vanadium monosulfide," *The Journal of chemical physics* **132**, 234304 (2010).
- ¹¹⁸T. C. Steimle, D. F. Nachman, J. E. Shirley, and A. J. Merer, "The permanent electric dipole moment of iron monoxide," *The Journal of chemical physics* **90**, 5360–5363 (1989).
- ¹¹⁹F. Wang and T. C. Steimle, "Communication: Electric dipole moment and hyperfine interaction of tungsten monocarbide, WC," (2011).
- ¹²⁰B. Sauer, J. Wang, and E. Hinds, "Laser-rf double resonance spectroscopy of ^{174}YbF in the X $^2\Sigma^+$ state: Spin-rotation, hyperfine interactions, and the electric dipole moment," *The Journal of chemical physics* **105**, 7412–7420 (1996).
- ¹²¹D. D. Nelson Jr, A. Schiffman, and D. J. Nesbitt, "The dipole moment function and vibrational transition intensities of OH," *The Journal of chemical physics* **90**, 5455–5465 (1989).
- ¹²²J. Shirley, C. Scurlock, T. Steimle, B. Simard, M. Vasseur, and P. Hackett, "Molecular beam optical Stark spectroscopy of YF," *The Journal of chemical physics* **93**, 8580–8585 (1990).
- ¹²³J. Hoelt, F. Lovas, E. Tiemann, R. Tischer, and T. Törring, "Elektrisches Dipolmoment und Mikrowellenrotationsspektrum von SnO, SnS, PbO und PbS," *Zeitschrift für Naturforschung A* **24**, 1222–1226 (1969).
- ¹²⁴P. Schwerdtfeger, J. S. McFeaters, M. J. Liddell, J. Hrušák, and H. Schwarz, "Spectroscopic properties for the ground states of AuF, AuF $^+$, AuF $_2$, and Au $_2$ F $_2$: A pseudopotential scalar relativistic Morner-Plesset and coupled-cluster study," *The Journal of chemical physics* **103**, 245–252 (1995).
- ¹²⁵T. Okabayashi, F. Koto, K. Tsukamoto, E. Yamazaki, and M. Tanimoto, "Pure rotational spectrum of gold monoxide (AuO) in the X $^2\Pi_{3/2}$ state," *Chemical physics letters* **403**, 223–227 (2005).
- ¹²⁶A. J. Parsons, S. P. Gleason, and T. D. Varberg, "High-resolution spectroscopy of the a $^4\Sigma_{3/2}-X_1^2\Pi_{3/2}$ system of gold monosulphide in the near infrared," *Molecular Physics* **116**, 3547–3553 (2018).
- ¹²⁷P. Bernath, R. Field, B. Pinchemel, Y. Lefebvre, and J. Schamps, "Laser spectroscopy of CaBr: A $^2\Pi-X^2\Sigma^+$ and B $^2\Sigma^+-X^2\Sigma^+$ systems," *Journal of Molecular Spectroscopy* **88**, 175–193 (1981).
- ¹²⁸P. Sheridan, M. Brewster, and L. M. Ziurys, "Rotational rest frequencies for CrO (X $^5\Pi_r$) and CrN (X $^4\Sigma^-$)," *The Astrophysical Journal* **576**, 1108 (2002).
- ¹²⁹J. F. Harrison, "Electronic structure of the transition metal nitrides TiN, VN, and CrN," *The Journal of Physical Chemistry* **100**, 3513–3519 (1996).
- ¹³⁰J. H. Bartlett, I. O. Antonov, and M. C. Heaven, "Spectroscopic and theoretical investigations of ThS and ThS $^+$," *The Journal of Physical Chemistry A* **117**, 12042–12048 (2013).
- ¹³¹T. Dunn, L. K. Hanson, and K. A. Rubinson, "Rotational analysis of the red electronic emission system of titanium nitride," *Canadian Journal of Physics* **48**, 1657–1663 (1970).

- ¹³²A. Douglas and P. Veillette, "The electronic spectrum of TiN," *The Journal of Chemical Physics* **72**, 5378–5380 (1980).
- ¹³³W. J. Balfour, A. J. Merer, H. Niki, B. Simard, and P. A. Hackett, "Rotational, fine, and hyperfine analyses of the (0, 0) band of the $D^3\Pi-X^3\Delta$ system of vanadium mononitride," *The Journal of chemical physics* **99**, 3288–3303 (1993).
- ¹³⁴B. Simard, C. Masoni, and P. Hackett, "Spectroscopy and photophysics of refractory molecules at low temperature: The $d^1\Sigma^+-X^3\Delta_1$ intercombination system of vanadium nitride," *Journal of Molecular Spectroscopy* **136**, 44–55 (1989).
- ¹³⁵A. J. Merer, "Spectroscopy of the diatomic 3d transition metal oxides," *Annual Review of Physical Chemistry* **40**, 407–438 (1989).
- ¹³⁶R. Ram and P. Bernath, "High-resolution fourier-transform emission spectroscopy of the $A^4\Pi-X^4\Sigma^-$ system of WN," *Journal of the Optical Society of America B* **11**, 225–230 (1994).
- ¹³⁷"See supplemental material at [url will be inserted by publisher]."
- ¹³⁸S. Hou, A. H. Qureshi, and Z. Wei, "Atomic charges in highly ionic diatomic molecules," *ACS Omega* **3**, 17180–17187 (2018).
- ¹³⁹M. Allen, D. Poggiali, K. Whitaker, T. R. Marshall, and R. Kievit, "Raincloud plots: a multi-platform tool for robust data visualization," *PeerJ Preprints* **6**, e27137v1 (2018).
- ¹⁴⁰C. D. Clark, "XLI. the application of a modified Morse formula to simple hydride diatomic molecules (Di-atoms)," *The London, Edinburgh, and Dublin Philosophical Magazine and Journal of Science* **19**, 476–485 (1935).
- ¹⁴¹C. D. Clark and J. L. Stoves, "Interrelation of dissociation energy and internuclear distance for some simple Di-atoms in ground states," *Nature* **144**, 285 (1939).
- ¹⁴²C. H. D. Clark, "Systematics of band-spectral constants. Part VII. The empirical form of relations involving group number," *Trans. Faraday Soc.* **37**, 299–302 (1941).
- ¹⁴³C. H. D. Clark and K. R. Webb, "Systematics of band-spectral constants. Part VI. Interrelation of equilibrium bond constant and internuclear distance," *Trans. Faraday Soc.* **37**, 293–298 (1941).
- ¹⁴⁴W. Gordy, "A relation between bond force constants, bond orders, bond lengths, and the electronegativities of the bonded atoms," *The Journal of Chemical Physics* **14**, 305–320 (1946).
- ¹⁴⁵K. M. Guggenheimer, "New regularities in vibrational spectra," *Proceedings of the Physical Society* **58**, 456–468 (1946).
- ¹⁴⁶W. Gordy, "A relation between characteristic bond constants and electronegativities of the bonded atoms," *Phys. Rev.* **69**, 130–131 (1946).
- ¹⁴⁷G. Herzberg, "Molecular spectroscopy: a personal history," *Annu. Rev. Phys. Chem.* **36**, 1 (1985).
- ¹⁴⁸R. S. Mulliken, "Electronic population analysis on LCAO-MO molecular wave functions. I," *The Journal of Chemical Physics* **23**, 1833–1840 (1955).
- ¹⁴⁹X. Liu, S. Truppe, G. Meijer, and J. Pérez-Ríos, "The Diatomic Molecular Spectroscopy Database," <https://rios.mp.fhi.mpg.de/index.php>, accessed February 1, 2020.
- ¹⁵⁰L. C. Krisher and W. G. Norris, "Microwave spectrum of silver bromide," *The Journal of Chemical Physics* **44**, 974–976 (1966).
- ¹⁵¹E. Herbst and W. Steinmetz, "Dipole moment of ICl," *The Journal of Chemical Physics* **56**, 5342–5346 (1972).
- ¹⁵²A. Hebert and C. Hollowell, "The radiofrequency spectra of LiF by the molecular beam electric resonance method," *The Journal of Chemical Physics* **65**, 4327–4327 (1976).
- ¹⁵³E. A. Scarl and F. Dalby, "High-field Stark effects on the near ultraviolet spectrum of the hydroxyl radical," *Canadian Journal of Physics* **49**, 2825–2832 (1971).